EurJIC
European Journal of Inorganic Chemistry

Research Article
doi.org/10.1002/ejic.202200767

Chemistry Europe
European Chemical Societies Publishing

www.eurjic.org

The Search for Enhanced σ-Donor Ligands to Stabilize Boron-Boron Multiple Bonds

Daniel E. Trujillo-González,[a, b] Gerardo González-García,[a] Trevor A. Hamlin,[c] F. Matthias Bickelhaupt,[c, d, e] Holger Braunschweig,[f, g] J. Oscar C. Jiménez-Halla,*[a] and Miquel Solà*[b]

Boron-boron multiple bonds, such as those found in diborenes and diborynes, are typically stabilized by σ-donor ligands that furnish electron density to these otherwise electron-deficient species. These compounds are not only of fundamental importance in the study of chemical bonding, but can also activate small molecules in a chemistry reminiscent of that carried out by transition metals. In the pursuit of designing new and improved σ-donor ligands to stabilize diborenes and diborynes suitable to activate small molecules, we performed density functional calculations to evaluate the Lewis basicity of a series of σ-donor ligands. For this evaluation, we analysed the interaction between the boranes and the σ-donor ligands in model systems L→BX_3 (X=F and Me) using energy decomposition analyses. We found that electronic bond energies of the L→BX_3 adducts correlate well with the ionization energies of the ligands and that ligands with high or medium basicity stabilize diborynes better than ligands with low basicity. We also learnt that beryllium-based ligands are promising since they are able to stabilize L→B≡B←L diborynes without significantly reducing the triple bond character of the B≡B bond.

Introduction

The study of main-group elements that behave similarly to transition metals (TMs) to fixate CO_2, to react with small molecules such as H_2, NH_3, C_2H_4 or CO, and to activate C–H and C–C bonds under mild conditions, has witnessed major advances in the last decades.[1–6] Main-group catalysts generally operate under mild conditions which may reduce the environmental impact,[2] have a reduced toxicity, and are overall cheaper than chemical processes associated to TM catalysis.[7,8] Bertrand and co-workers nicely showcased H_2 activation by (alkyl)(amino)carbenes at 35 °C.[9] Similarly, Power and coworkers[10] achieved H_2 activation with Ga_2Ar_2 (Ar = 2,6-(2,6-i$Pr_2C_6H_3$)2-4-(Me_3Si)C_6H_2) at 25 °C and 1 atm. On the other hand, H_2 was produced from the reduction of water or alcohols with potassium-graphite, C_8K.[11] Moreover, C–C bond activation was observed by Inoue and co-workers with a dialumene ((NHC)(tBu_2MeSi)Al=Al(SiMetBu_2)(NHC)) (NHC = N-heterocyclic carbene) (see Figure 1)[12] and by Cowley and co-workers using a phosphaborene at 80 °C.[13] In this context, let us mention that Liu et al. have recently synthesised a free phosphaborene stable at room temperature.[14]

Species containing boron are among the most investigated in the search for metallomimetic compounds based on main-group elements.[2] Boron is often featured in frustrated Lewis pairs (FLPs) that are particularly efficient as metal-free catalysts

[a] D. E. Trujillo-González, Dr. G. González-García, Dr. J. O. C. Jiménez-Halla
Departamento de Química
Universidad de Guanajuato
Campus Guanajuato
Noria Alta S/N, CP 36050, Guanajuato, Gto (México)
E-mails:
E-mail: jjimenez@ugto.mx
[b] D. E. Trujillo-González, Prof. Dr. M. Solà
Institut de Química Computacional i Catàlisi
and Departament de Química
Universitat de Girona
C/ Maria Aurèlia Capmany, 69
17003 Girona, Catalonia (Spain)
E-mail: miquel.sola@udg.edu
[c] Dr. T. A. Hamlin, Prof. Dr. F. M. Bickelhaupt
Department of Theoretical Chemistry
Amsterdam Institute of Molecular and Life Sciences (AIMMS)
Amsterdam Center for Multiscale Modeling (ACMM)
Vrije Universiteit Amsterdam
De Boelelaan 1083
1081 HV Amsterdam (The Netherlands)
[d] Prof. Dr. F. M. Bickelhaupt
Institute of Molecules and Materials
Radboud University
Heyendaalseweg 135, 6525 AJ Nijmegen (The Netherlands)
[e] Prof. Dr. F. M. Bickelhaupt
Department of Chemical Sciences
University of Johannesburg
Auckland Park, Johannesburg 2006 (South Africa)
[f] Prof. Dr. H. Braunschweig
Institute for Inorganic Chemistry
Julius-Maximilians-Universität Würzburg
97074 Würzburg (Germany)
[g] Prof. Dr. H. Braunschweig
Institute for Sustainable Chemistry & Catalysis with Boron
Julius-Maximilians-Universität Würzburg
97074 Würzburg (Germany)

Supporting information for this article is available on the WWW under https://doi.org/10.1002/ejic.202200767

Research Article
doi.org/10.1002/ejic.202200767

Chemistry Europe
European Chemical Societies Publishing

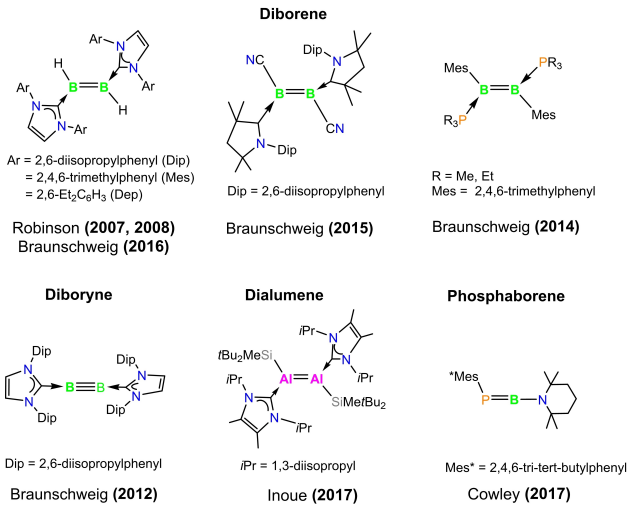

Figure 1. Selected examples of compounds with Al–Al, P–B and B–B multiple bonds.

able to activate small molecules.[15–19] Furthermore, in situ generated mono- and dicoordinated borylenes react with alkynes, CO, and N_2 and activate C–H and C–C[20] bonds in a chemistry reminiscent of that carried out by TMs.[2,21] Finally, species with boron-boron multiple bonds (such as diborenes and diborynes, see Figure 1)[22] can bind small molecules (CO, CO_2) and activate bonds like TMs do,[2,23] taking part as catalysts in catalytic cycles.[24]

The first neutral diborene was synthesized by Robinson and co-workers. They reduced a boron trihalide stabilized by : $C\{N(2,6\text{-}iPr_2C_6H_3)CH\}_2$ using potassium graphite at room temperature to obtain a mixture of diborenes and diboranes.[25,26] On the other hand, the dicarbonyl adduct OC:→B≡B←:CO was the first experimentally detected diboryne.[27,28] To stabilize compounds with BB multiple bonds, it is necessary to fill the empty $2p_z$ orbital on each boron atom using a σ-donor ligand that donates an electron pair (see Figure 1).[2,25,26,29–38] Another strategy to stabilize group 13 multiple bonding is through electronic transmutation as used by Boldyrev, Bowen, and Zhang.[39–41]

It is worth noting that the coordination of σ-donor ligands stabilizes the B=B and B≡B multiple bonds in diborenes and diborynes, but it could also reduce their capability to activate small molecules.[34,35] The same is also true for diboraallenes and diboratriazoles, which have been stabilized with PMe_3 and (alkyl)(amino)carbene ligands.[42] Here, we hypothesize that strong σ-donors stabilize boron-boron multiple bonds but reduce the Lewis acidity of the boron atoms making these systems less efficient for catalysis, whereas weak σ-donors may not sufficiently stabilize diborenes and diborynes, leading to decomposition and ruling out their use as catalysts. As such, we are interested in identifying optimal σ-donor ligands that are neither too strong nor too weak that could be used in the next generation of catalytic diborenes and diborynes.

The basic character of a σ-donor ligand can be quantified by analysing its interaction with a Lewis base. In our study, the basicity of a series of the σ-donor ligands will be analysed from the strength of the chemical bond formed in the interaction with boranes, i.e., in model systems $L{\rightarrow}BX_3$ (X=F and Me). This is a classical textbook example of a donor-acceptor interaction that have been studied in several works. Frenking et al. studied the interaction between diaminocarbene $C(NH_2)_2$, NH_3, and CO with the Lewis acids EF_3 and ECl_3 (E=B, Al, Ga, In). They found that the dissociation energy of the $X_3E{-}CO$, $X_3E{-}NH_3$, and $X_3E{-}C(NH_2)_2$ (X=F, Cl) adducts increases from boron to the heavier Group 13 elements.[43] Hamlin and co-workers[44] studied the interaction between boranes (BX_3, Lewis acids) and amines (NY_3, Lewis bases, with X, Y=H, F, Cl, Br, I), using the activation strain model (ASM) to decompose the bond energy into strain and interaction energy (see below). They found that the bond strength in $H_3B{-}NY_3$ species increases when then energy of the HOMO of the base increases, i.e., $\Delta E(NI_3) > \Delta E(NBr_3) > \Delta E(NCl_3) > \Delta E(NF_3)$,[44] because of the enhanced $HOMO_{NY3}$—$LUMO_{BX3}$ interaction (Scheme 1). Lein and Frenking studied the interaction between boranes-amines and boranes-phosphines analysing the interaction energy (ΔE_{int}) rather than the bond dissociation energy. They found that the absolute value of the ΔE_{int} term in $X_3B{-}EY_3$ (X, Y=Cl, Me and H; E=N, P) increases in the order $EMe_3 > EH_3 > ECl_3$ (E=N, P) and correlates with a reduction in the electrostatic interaction (ΔV_{elstat}).[45]

In our study, we selected two boranes with different electron accepting abilities (BF_3 and BMe_3) to analyse the basicity of several ligands (see Figure 2) that are used in the p block chemistry and organometallic chemistry. As for the Lewis bases, we have judiciously selected ligands with a varying degree of σ-donor character with the aim of analysing different σ-donor ligands that could stabilize boron-boron multiple bonds. Some of them (NH_3, H_2O, pyridine, and PMe_3) were selected because experimental data of the $L{\rightarrow}BX_3$ interaction is available. Simplified models of (2,6-diisopropylphenyl)-3,3,5,5-tetramethylpyrrolidin-2-ylidene (CAAC) and 1,3-bis(2,6-diisopropylphenyl)-1,3-dihydro-2H-imidazol-2-ylidene (NHC) ligands were chosen for the same reason and because they are the typical ligands that stabilize diborenes and diborynes. In these simplified models, we substituted the 2,6-diisopropylphenyl (Dip) groups by H atoms to reduce the computational cost. As an additional carbene, we considered the phosphino(sylyl)carbene (PSC).[46] We also include some important borylenes like mesitylborylene (BMes) and mesitylpyridineborylene (BMpyr) as well as hydrogen cyanide (HCN), hydrogen isocyanide (HNC) and, finally, some ligands with Be atoms, namely, beryllium trisdimethylamine ($Be(NHMe_2)_3$) and

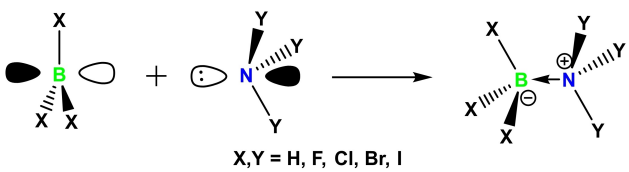

Scheme 1. Interaction between the LUMO of a borane and the HOMO of an amine that leads to the formation of the Lewis acid/base adduct.

Research Article
doi.org/10.1002/ejic.202200767

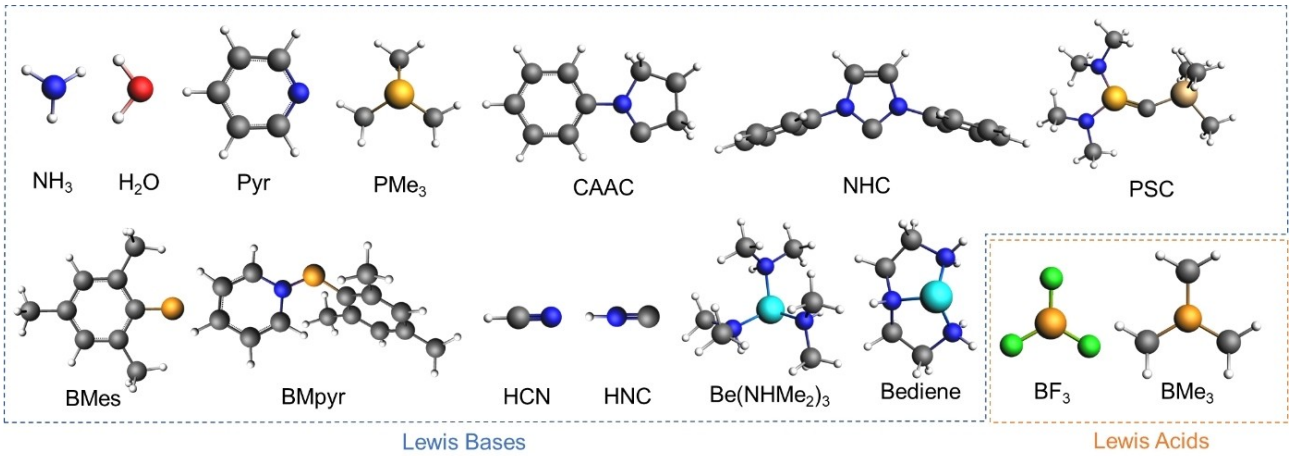

Figure 2. Ligands and boranes studied in this work. Grey: C, aqua: Be, white: H, blue: N, red: O, green: F, amber: P, orange: B, khaki: Si.

beryllium diethylenetriamine (Bediene). The latter were chosen because this type of Be compounds has been used as Lewis bases in previous studies.[47,48] Other ligands not used in experiments involving species with multiple boron-boron bonds, such as dimethyl sulfoxide (DMSO)[49] and thiophene, were also considered but these species dissociate during geometry optimizations, whereas CO binds to trimethylborane (with an electronic bond dissociation energy of 17.6 kcal/mol) but not to trifluoroborane. For all these cases, we did not consider these ligands since they did not form the expected coordinated species and we concluded that they will not stabilize diborenes and diborynes.

Computational Methods

All density functional theory (DFT) calculations were performed with the hybrid PBE0[50] functional using the Amsterdam Density Functional (ADF2019) software package.[51,52] The all-electron basis set used, denoted TZ2P, is of triple-ζ quality with two sets of polarization functions for all atoms. In all cases, standard convergence criteria and a fine grid were used. Dispersion forces were included via Grimme's dispersion correction scheme (DFT-D3(BJ)),[53] which contains the damping function proposed by Becke and Johnson.[54] All optimized stationary points were verified by performing a vibrational analysis calculation, to be energy minima (no imaginary frequencies). The bond dissociation energy ($-\Delta E_{BDE}$) was calculated from the gas-phase electronic energies (Eq. (1)):[55–58]

$$-\Delta E_{BDE} = E_{adduct} - E_{ligand} - E_{borane} \quad (1)$$

Enthalpies at 298.15 K and 1 atmosphere (ΔH_{298}) were calculated from electronic energies (ΔE) and vibrational frequencies using standard thermochemistry relations for an ideal gas, according to Equation (2):[11]

$$\Delta H_{298} = \Delta E + \Delta E_{trans,298} + \Delta E_{rot,298} + \Delta E_{vib,0} + \Delta(\Delta E_{vib,0})_{298} + \Delta(pV) \quad (2)$$

Here, $\Delta E_{trans,298}$, $\Delta E_{rot,298}$, and $\Delta E_{vib,0}$ are the differences between the reactant and products in translational, rotational, and zero-point vibrational energy, respectively. $\Delta(\Delta E_{vib,0})_{298}$ is the change in the vibrational energy difference as one goes from 0 to 298.15 K. The molar work term $\Delta(pV)$ is $(\Delta n)RT$; $\Delta n = +1$ for one reactant dissociating into the two products. Thermal corrections for the electronic energy are neglected. The bond dissociation enthalpy ($-\Delta H_{BDE}$) and bond dissociation Gibbs energy ($-\Delta G_{BDE}$) can be computed using Equations 3 and 4:

$$-\Delta H_{BDE} = H_{adduct} - H_{ligand} - H_{borane} \quad (3)$$

$$-\Delta G_{BDE} = G_{adduct} - G_{ligand} - G_{borane} \quad (4)$$

For the reported ΔH_{BDE} and ΔG_{BDE}, we have incorporated solvent effects of a dichloromethane (DCM) solution by means of the COSMO model.[59]

Using the activation strain model (ASM),[55–58] the bond dissociation energy can be decomposed, along the reaction coordinate ξ, into two physically meaningful terms (Eq. (5)):

$$-\Delta E_{BDE}(\xi) = \Delta E_{strain}(\xi) + \Delta E_{int}(\xi) \quad (5)$$

Here, the strain energy, ΔE_{strain}, is the amount of energy required to deform the fragments from their equilibrium structure to the geometry that they acquire in the overall complex. The interaction energy, ΔE_{int}, corresponds to the actual energy change when the geometrically deformed fragments are combined to form the overall complex. ΔE_{int} can further be decomposed within the framework of the canonical Kohn-Sham molecular orbital (MO) model by means of our energy decomposition analysis (EDA) (Eq. (6)):[55–58,60]

Research Article
doi.org/10.1002/ejic.202200767

$$\Delta E_{int}(\xi) = \Delta V_{elstat}(\xi) + \Delta E_{Pauli}(\xi) + \Delta E_{oi}(\xi) + \Delta E_{dis}(\xi) \quad (6)$$

The term ΔV_{elstat} corresponds to the classical electrostatic interaction between the unperturbed charge distributions of the fragments in the geometry they possess in the complex. This term is usually attractive. The Pauli-repulsion, ΔE_{Pauli}, between these fragments comprises the destabilizing interactions, associated with the Pauli-principle for fermions, between occupied orbitals and is responsible for the steric repulsion. The orbital interaction, ΔE_{oi}, between these fragments in any MO model, and therefore also in Kohn-Sham theory, accounts for bond pair formation, charge transfer (empty/occupied orbital mixing between different fragments) and polarization (empty/occupied orbital mixing on one fragment due to the presence of another fragment). Lastly, the ΔE_{disp} term accounts for attractive dispersion interactions.

To verify some of our results, domain-based local pair natural orbital coupled cluster[61,62] (DLPNO-CCSD(T)/def2-TZVPPD) calculations were performed using ORCA.[63]

Moreover, the hardness was calculated using Equation (7):[64]

$$\eta = (E_{N-1} + E_{N+1} - 2E_N)/2 \quad (7)$$

where E_N is the total energy of neutral and E_{N-1} and E_{N+1} are the energy of the cationic and anionic systems at the geometry of the neutral species. Additionally, we obtained the bond order in diborynes using the Mayer bond order (MBO) formulation.[65]

Results and Discussion

We have divided our analysis into two sections, one for each borane considered.

BF_3 adducts. We studied twelve adducts whose X–B bond lengths and θ_{XBF} angles (see Figure 3) are in accordance with the results reported in the literature for some of the complexes: CAAC→BF_3 (*expt.* 1.674 Å[66]), NHC→BF_3 (*expt.* 1.656 Å[67]), pyr→BF_3 (*expt.* 1.669 Å;[68] *expt.* 1.604 Å and 107.3°[69]), H_3N→BF_3 (*theor.* 1.620 Å;[70] *expt.* 1.600 Å;[70] *theor.* 1.720 Å[44]), Me_3P→BF_3 (*expt.* 2.029 Å[71]), and H_2O→BF_3 (*expt.* 1.532 Å;[72] *theor.* 1.790 Å;[73] *theor.* 1.814 Å and 99.4°[74]) with a standard deviation with respect to experimental values for B–X bond lengths of ±0.098 Å (±0.027 Å if we exclude the water ligand) and a difference of 1.5° for the $\measuredangle_{OBF}$ angle of pyr→BF_3. The HCN→BF_3 adduct was not studied because is not stable. The boron-beryllium bond length varies from 1.914 to 1.920 Å and the boron-carbon bond length from 1.670 to 1.816 Å. The boron-boron bond lengths are 1.746 and 1.755 Å for BMpyr and BMes, respectively, while boron-nitrogen bonds are 1.661 and 1.672 Å for pyridine and ammonia. The boron-oxygen and boron-phosphorus bonds lengths are 1.791 Å and 2.063 Å for water and trimethylphosphine, respectively. As expected, the pyramidalization angle[75] of BF_3 is higher for bulkier ligands ($Be(NHMe_2)_3$, Bediene, BMpyr, CAAC, and NHC) than for the less bulky ligands (H_2O, NH_3, and HNC) (see Table S1).

As can be seen in Figure 3, the bond dissociation energy ($-\Delta E_{BDE}$) in gas-phase increases in the order: $Be(NHMe_2)_3$ > Bediene > BMpyr > CAAC > NHC > PSC > BMes > pyr > NH_3 > PMe_3 > H_2O > HNC. According to these results, we can classify

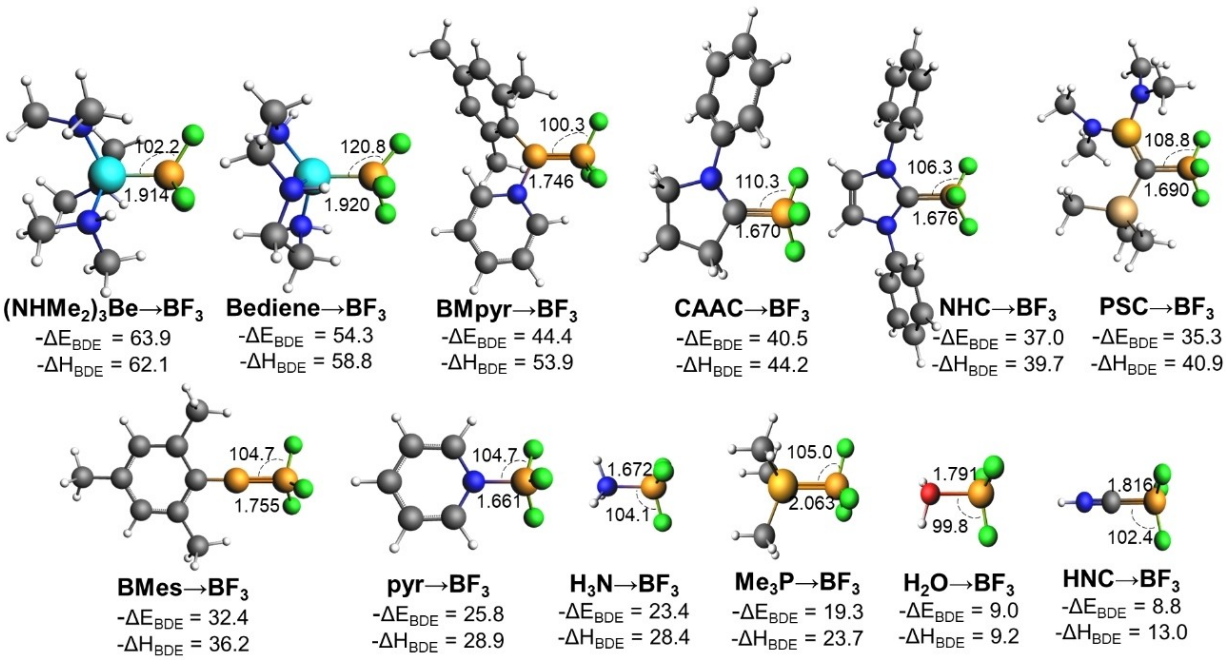

Figure 3. Optimized geometries of the L→BF_3 complexes. Dative bond (R_e) distances are shown in Å, L-B-F angles (∡) are in degrees, bond dissociation energies ($-\Delta E_{BDE}$) in gas-phase and the bond dissociation enthalpies ($-\Delta H_{BDE}$) in DCM are in kcal/mol. Grey: C, aqua: Be, white: H, blue: N, red: O, green: F, amber: P, orange: B, khaki: Si.

Research Article
doi.org/10.1002/ejic.202200767

$Be(NHMe_2)_3$, Bediene, and BMpyr as strong Lewis bases, CAAC, NHC, PSC, and BMes as intermediate Lewis bases, and pyr, NH_3, PMe_3, H_2O, and HNC as weak Lewis bases. Obviously, the classification of ligands in these three groups is not strict and it could be done using other criteria. Except for $Be(NHMe_2)_3$, calculated $-\Delta H_{BDE}$ in DCM are somewhat larger than in gas-phase but trends in Lewis basicity remain the same except for PSC (which becomes slightly stronger than NHC likely because of the higher dipole moment of PSC→BF_3 as compared to NHC→BF_3) and HNC (which becomes stronger than H_2O, for the same reason). For some ligands, calculated $-\Delta H_{BDE}$ in DCM can be compared with experimental values obtained in DCM: pyr→BF_3 30.6 kcal/mol, Me_3P→BF_3 23.3 kcal/mol,[76] H_3N→BF_3 25.5 kcal/mol, and H_2O→BF_3 11.2 kcal/mol.[77] When compared to experimental values, errors in calculated $-\Delta H_{BDE}$ are found to be always lower than 3.0 kcal/mol and, on average, our calculated results are only 1.6 kcal/mol lower than the experimental values, showing the reliability of our approach to obtain $-\Delta H_{BDE}$. The accuracy of the results is further checked by computing the gas-phase BDEs of three of the smallest adducts at the DBLPNO-CC/def2-TZVPPD level of theory. The PBE0-D3(BJ)/TZ2P results for the $-\Delta E_{BDE}$ of pyr→BF_3, H_3N→BF_3, and H_2O→BF_3 differ by less than 1.3 kcal/mol from those obtained with the DLPNO-CCSD(T)/def2-TZVPPD method (see Table S8).

EDA analysis shown in Figure 4 (for more details see Table S2), indicates that the interaction energy, ΔE_{int}, is the major contributor to the $-\Delta E_{BDE}$. However, ΔE_{strain} is not negligible, in particular, the deformation of the BF_3 fragment. As shown by Hamlin and coworkers,[44] ΔE_{strain} increases for the adducts formed with bulky ligands that leads to an increased degree of pyramidalization of BF_3, which costs significant energy to deform the strong B–F bonds (Table S1). With respect to the different components of ΔE_{int}, the Pauli repulsion for $Be(NHMe_2)_3$ and Bediene adducts is above 200 kcal/mol, for BMpyr, CAAC, NHC, PSC, BMes, pyr, NH_3, and PMe_3 adducts, the ΔE_{Pauli} values range from 121.0 to 182.0 kcal/mol, and, finally, for the H_2O and HNC adducts are 70.0 and 93.0 kcal/mol, respectively. In general, the Pauli repulsion increases with the size of the ligands. Contribution of the electrostatic and orbital interaction terms to ΔE_{int} is similar, with the ΔV_{elstat} values being somewhat more stabilizing than the orbital interactions, except for Bediene→BF_3 and BMpyr→BF_3 adducts (in these cases, the ΔE_{oi} represents 53% and 52% of the attractive part ($\Delta V_{elest}+\Delta E_{oi}$), respectively). The ΔV_{elstat} in $Be(NHMe_2)_3$, CAAC, NHC, PSC, BMes, pyr, NH_3, PMe_3, H_2O, and HNC adducts vary from −203.0 to −51.0 kcal/mol. Finally, the dispersion energy, which is stabilizing by about 1 to 4 kcal/mol, has a minor contribution. For the adduct H_3N→BF_3, ΔE_{Pauli} is 125.1 kcal/mol, ΔV_{elstat} is −88.8 kcal/mol, and ΔE_{oi} is −81.5 kcal/mol, which qualitatively agrees with previous results reported by some of us (133.6 kcal/mol, −94.5 kcal/mol, and −77.1 kcal/mol, respectively).[44] By forcing the C_s or C_{3v} symmetry in Bediene, NHC, BMes, pyr, NH_3, PMe_3, H_2O and HNC, we can separate ΔE_{oi} into their ΔE_σ and ΔE_π components (see Table S4). Symmetrisation does not lead to significant changes neither in the geometries nor in the $-\Delta E_{BDE}$ except for Bediene→BF_3 (49.7 after symmetrisation vs. 54.3 kcal/mol). In fact, after symmetrisation, the $-\Delta E_{BDE}$ trend remains unchanged. We found that, in all cases, the ΔE_σ term is the most important, the contributions of ΔE_π ranging from 1% (Bediene) to 11% (HCN). The largest contribution of ΔE_π to the dissociation energy corresponds to the Me_3P→BF_3 adduct with $\Delta E_\pi = -6.4$ kcal/mol.

BMe_3 adducts. We studied eleven adducts for this case. The BMes→BMe_3 and BMpyr→BMe_3 complexes were not considered because during the optimization process a Me fragment from BMe_3 migrated to the borylene boron atom. Our results (see Figure 5) agree with the values reported in the literature for NHC→BMe_3 (*expt.* 1.688 Å[78]), pyr→BMe_3 (*expt.*

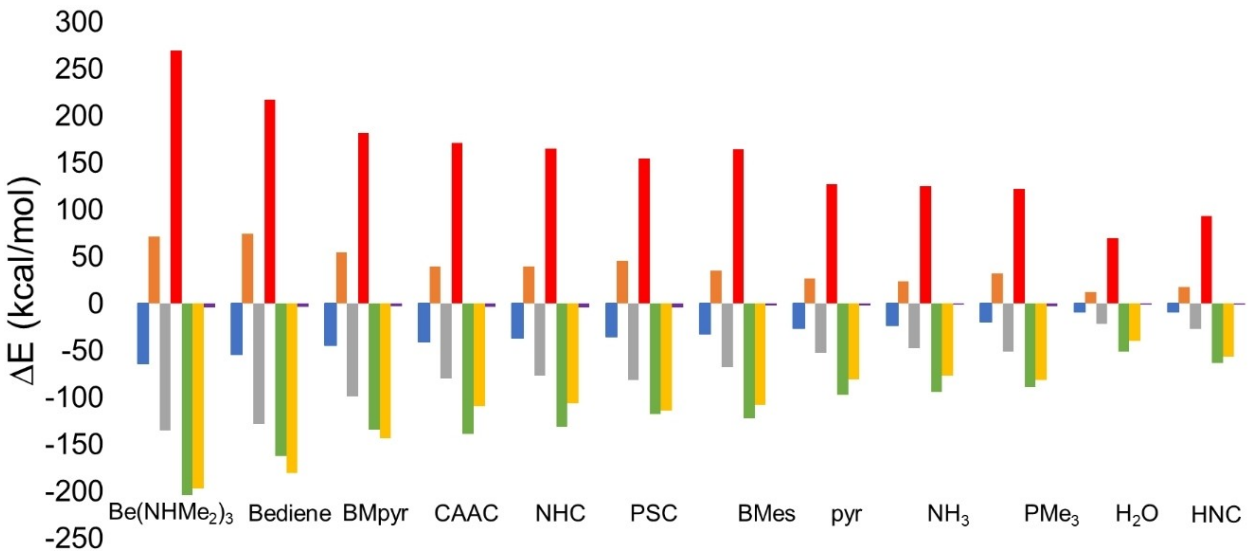

Figure 4. Energy decomposition analysis for L→BF_3: $-\Delta E_{BDE}$ (blue), ΔE_{strain} (orange), ΔE_{int} (gray), ΔE_{Pauli} (red), ΔV_{elstat} (green), ΔE_{oi} (yellow) and ΔE_{dis} (purple). The different L ligands considered are placed on the horizontal axis. The complexes are arranged left to right from higher to lower bond dissociation energy.

Research Article
doi.org/10.1002/ejic.202200767

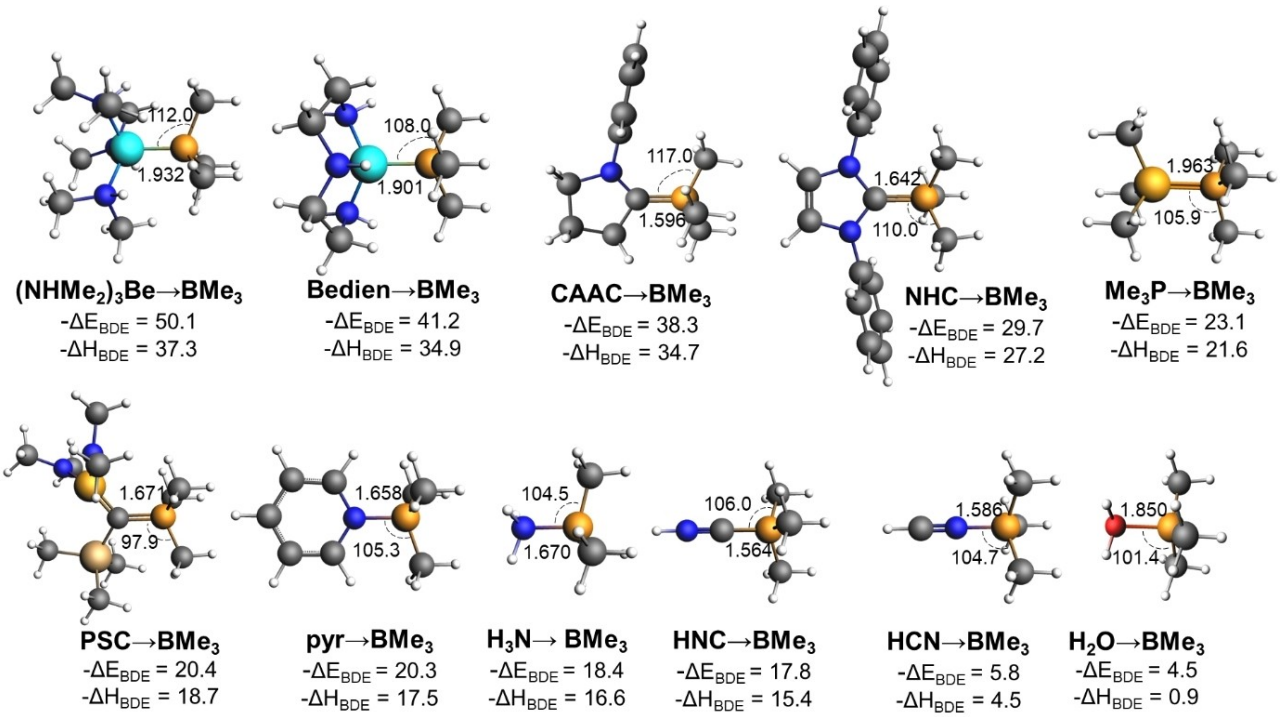

Figure 5. Optimized geometries for the L→BMe_3 complexes. Dative bond (R_e) distances are given in Å, L-B-F angles (∡) are in degrees, and bond dissociation energies ($-\Delta E_{BDE}$) in gas-phase and bond dissociation enthalpies ($-\Delta H_{BDE}$) in DCM are in kcal/mol. Grey: C, aqua: Be, white: H, blue: N, red: O, amber: P, orange: B, khaki: Si.

1.664 Å[79]), H_3N→BMe_3 (*expt.* 1.629 Å;[80] *theor.* 1.697 Å;[81] *theor.* 1.683 Å[82]), Me_3P→BMe_3 (*theor.* 1.989 Å;[82] *theor.* 2.014 Å;[81] *theor.* 1.989 Å[82]), and H_2O→BMe_3 (*theor.* 1.954 Å[83]) within a variation of ±0.022 Å on average with respect to the experimental values. The boron-beryllium bond lengths are 1.932 and 1.901 Å for $Be(NHMe_2)_3$ and Bediene, respectively. The bond lengths vary from 1.564 to 1.671 Å for carbon linked to boron. The boron-nitrogen bonds range from 1.586 to 1.670 Å. Finally, the boron-oxygen and boron-phosphorus bonds lengths are 1.850 Å and 1.963 Å, respectively. As above, the pyramidalization BMe_3 angle tends to be higher when we use bulkier ligands ($Be(NHMe_2)_3$, Bediene, CAAC, NHC) than smaller ligands such as H_2O, NH_3, and HNC. Except for L= $Be(NHMe_2)_3$, the L–B distance is always shorter for BMe_3 than for BF_3 complexes.

L→BMe_3 adducts exhibit an increase in the gas-phase bond dissociation energies ($-\Delta E_{BDE}$) in the following order: $Be(NHMe_2)_3$ > Bediene > CAAC > NHC > PMe_3 > PSC > pyr > NH_3 > HNC > HCN > H_2O (see Figure 6 and Table S3). PBE0-D3(BJ)/TZ2P results for the gas-phase bond dissociation energies of H_3N→BMe_3 and H_2O→BMe_3 differ by less than 0.5 kcal/mol from those obtained at the DBLPNO-CC/def2-TZVPPD (see Table S8). For the ligands shared by BF_3 and BMe_3, the ordering is the same but, contrary to what was found for BF_3, there is a significant reduction in the $-\Delta H_{BDE}$ when going from gas-phase to DCM solution that we attribute to the higher stabilization in DCM of BMe_3 as compared to BF_3 due to the gas-phase dipole moment of BMe_3 (0.3 D), whereas BF_3 has a zero-dipole moment. EDA shows that in the formation of L→BMe_3 adducts, the BMe_3 fragment deformation is the main contributor to the ΔE_{strain} (Table S3). The ΔE_{Pauli} in $Be(NHMe_2)_3$, Bediene, CAAC, and NHC adducts are above 170.0 kcal/mol. For PMe_3, PSC, pyr, NH_3, HCN, HNC, and H_2O adducts ΔE_{Pauli} ranges from 62.0 to 159.0 kcal/mol. In general, contributions from the ΔV_{elstat} and ΔE_{oi} are similar, the ΔV_{elstat} being somewhat more stabilizing, except in the Bediene→BMe_3, PSC→BMe_3, HNC→BMe_3, and HCN→BMe_3 adducts, where the orbital interaction energy is slightly more stabilizing than the electrostatic energy (ΔE_{oi} represents 50%, 52%, 53%, and 53% of the attractive part ($\Delta V_{elstat} + \Delta E_{oi}$) in each adduct, respectively). Our EDA results follow the same trends as previous reports. In the NH_3→BMe_3 adduct, ΔE_{Pauli} is 129.0 kcal/mol, ΔV_{elstat} is −90.3 kcal/mol and ΔE_{oi} is −74.7 kcal/mol that agree with Bessac and Frenking results (128.5 kcal/mol, −83.8 kcal/mol, and −65.1 kcal/mol, respectively).[44] For the Me_3P→BMe_3 complex, Skara et al. report ΔE_{Pauli} = 149.2 kcal/mol, ΔV_{elstat} = −92.5 kcal/mol and ΔE_{oi} = −93.6 kcal/mol,[84] while our results are 153.5, −96.3, and -95.5 kcal/mol, respectively. Also for BMe_3 adducts, we forced the C_{3v} or C_s symmetry in Bediene, NHC, BMes, pyr, NH_3, PMe_3, H_2O, HCN, and HNC, to split the ΔE_{oi} term into the ΔE_σ and ΔE_π contributions (see Table S5). Likewise the L→BF_3 adducts, the $-\Delta E_{BDE}$ trend does not change with the symmetrisation process. We found contributions of ΔE_π to ΔE_{oi} are generally minor and range between 2% (Bediene) and 20% (HCN). The H_2O→BMe_3 adduct has an ΔE_π of −1.5 kcal/mol, whereas for

Research Article
doi.org/10.1002/ejic.202200767

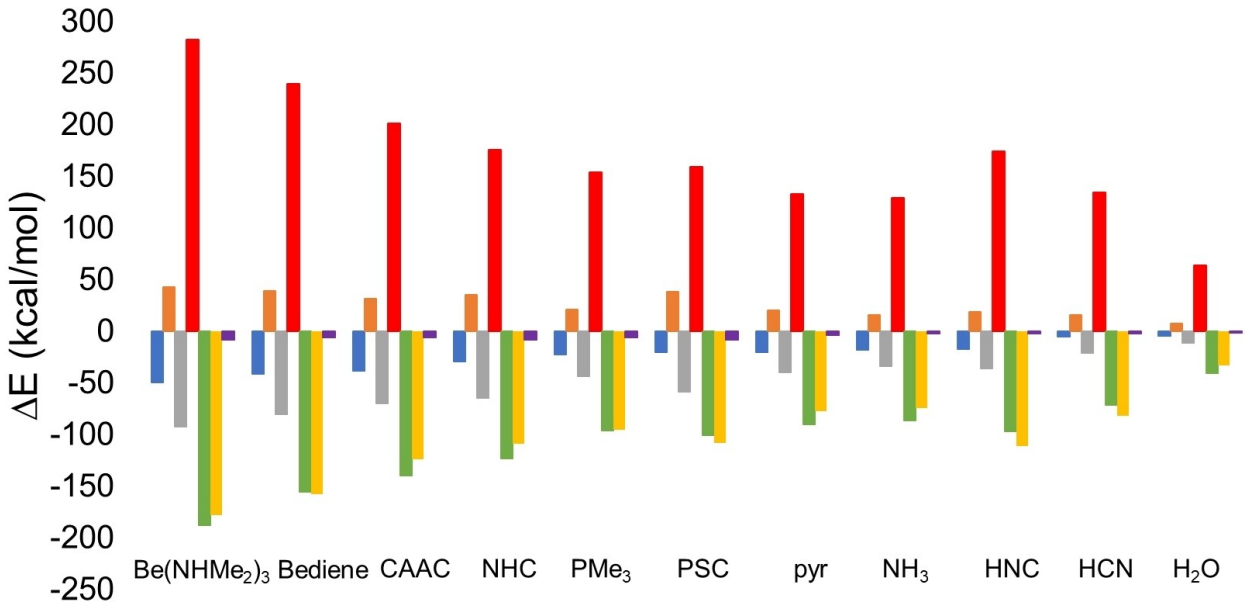

Figure 6. EDA for L→BMe_3: $-\Delta E_{BDE}$ (blue), ΔE_{strain} (orange), ΔE_{int} (gray), ΔE_{Pauli} (red), ΔV_{elstat} (green), ΔE_{oi} (yellow) and ΔE_{dis} (purple). The different L ligands considered are placed on the horizontal axis. The complexes are arranged left to right from higher to lower bond dissociation energy.

the HNC→BMe_3 adduct ΔE_π is −22.1 kcal/mol. Finally, the ΔE_π character for H_3N→BMe_3 is 10% and Me_3P→BMe_3 is 12%, both percents close to the ΔE_π contribution of 10% and 13%, respectively, reported by Lein and Frenking.[45]

As said before, despite having a longer L–B bond length, BF_3 adducts have higher $-\Delta E_{BDE}$ than BMe_3 adducts, exceptions being the ligands PSC and HNC. To find a reason for this behavior, we have performed the EDA along the reaction coordinate for the dissociation of the L→BX_3 complexes (see Figure S1). As an example, Figure 7 shows the results for the NHC→BX_3 complexes. As can be seen, NHC→BF_3 has higher ΔE_{strain} and more stabilizing ΔE_{int} than NHC→BMe_3 along the reaction coordinate. The difference in ΔE_{int} between NHC→BF_3 and NHC→BMe_3 complexes ($\Delta\Delta E_{int} = \Delta E_{int}(L{\rightarrow}BF_3) - \Delta E_{int}(L{\rightarrow}BMe_3)$) is, in absolute value, larger than the $\Delta\Delta E_{strain} = \Delta E_{strain}(L{\rightarrow}BF_3) - \Delta E_{strain}(L{\rightarrow}BMe_3)$. This is why, in general, L→BF_3 adducts have lower ΔE_{BDE} than L→BMe_3 ones. On the other hand, whereas $\Delta\Delta E_{int}$ remains more or less constant along the reaction coordinate, $\Delta\Delta E_{strain}$ increases for short distances. As a result, the L–B bond length in the equilibrium is shorter for L→BF_3 adducts. When analyzing the $\Delta\Delta E_{int}$ term, we find that the most important difference corresponds to the $\Delta\Delta V_{elstat}$ term, which is more stabilizing for L→BF_3 adducts than for L→BMe_3 ones. We attribute the more stabilizing ΔV_{elstat} values in

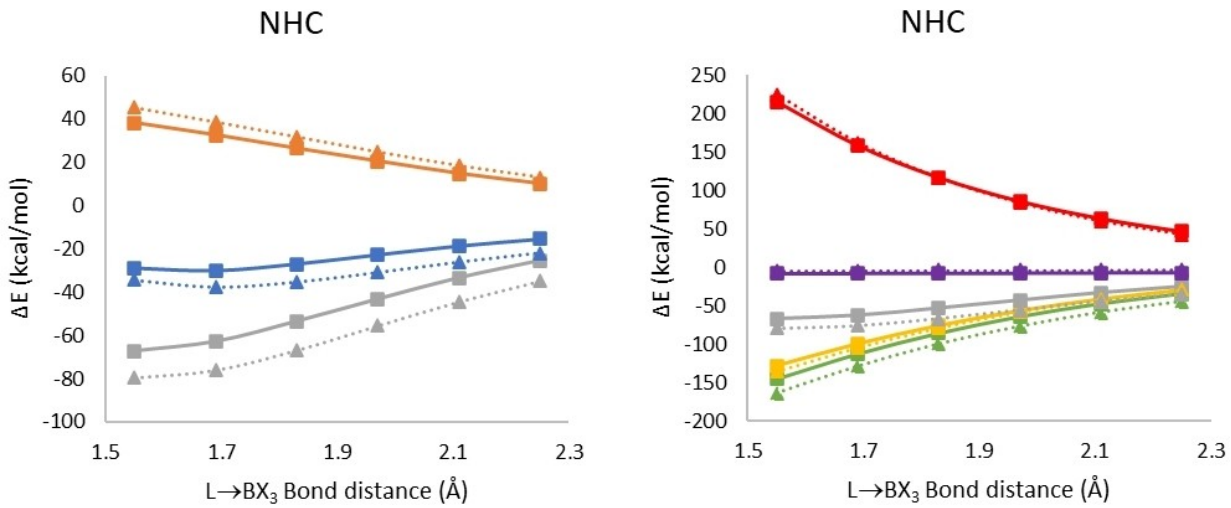

Figure 7. (left) Activation strain model and (right) energy decomposition analysis for NHC→BF_3 (triangle mark dot line) and NHC→BMe_3 (square mark straight line), calculated at PBE0-D3(BJ)/TZ2P. $-\Delta E_{BDE}$ (blue), ΔE_{strain} (orange), ΔE_{int} (gray), ΔE_{Pauli} (red), ΔV_{elstat} (green), ΔE_{oi} (yellow) and ΔE_{dis} (purple).

Research Article
doi.org/10.1002/ejic.202200767

$L{\rightarrow}BF_3$ adducts to the more polarized B–F bonds as compared to the B–CH_3 ones (see Tables S2 and S3). Finally, the ΔE_{oi} term is slightly more stabilizing in $NHC{\rightarrow}BF_3$ than in $NHC{\rightarrow}BMe_3$ because of the worse $HOMO_L$-$LUMO_{BMe3}$ interaction due to the increased $HOMO_L$-$LUMO_{BMe3}$ energy gap. Indeed, even though the $LUMO_{BF3}$ (0.2 eV) is higher than the $LUMO_{BMe3}$ (−0.3 eV), the $LUMO_{BF3}$ at the geometry of BF_3 in the adduct, i.e. $LUMO_{BF3adduct}$, is lower in energy than $LUMO_{BMe3adduct}$ (Table S7). Pyramidalization stabilizes the LUMO and destabilizes the HOMO of the BX_3 Lewis acids.[44] Finally, we have additionally analysed the $L{\rightarrow}BMe_3$ adducts at the optimized L–B distance of the $L{\rightarrow}BF_3$ adducts. Changes are minor and trends are the same as discussed above (see Table S6). As a whole and as pointed out by Hamlin and coworkers,[44] although the $HOMO_L$-$LUMO_{BX3}$ interaction is one of the most important stabilizing effects, in general, Lewis base/BX_3 interactions are a complex interplay of different energy components. A paradigmatic example is the $HNC{\rightarrow}BX_3$ complexes. The optimized C–B bond length is 1.816 Å in $HNC{\rightarrow}BF_3$ and 1.546 Å in $HNC{\rightarrow}BMe_3$. The important C–B bond length difference is due to a combination of an increase at short distances in both $\Delta\Delta E_{strain}$ and $\Delta\Delta E_{int}$, the latter being negative at long distances and positive at short distances. As a result, the equilibrium geometry of $HNC{\rightarrow}BMe_3$ is much shorter than in $HNC{\rightarrow}BF_3$. The reason for the important $\Delta\Delta E_{int}$ change is the increase in $\Delta\Delta E_{Pauli}$ and $\Delta\Delta E_{oi}$ components at short distances (see Figure S1).

Correlations between $-\Delta E_{BDE}$ and some electronic properties of the ligands and boranes were investigated to search for possible connections (see Figure 8). The first one is the correlation between the ionization energy of the ligand (IE) and $-\Delta E_{BDE}$. We associated the ionization energy with the capacity of a ligand to donate electron density to the borane fragment, so that lower IE values represent higher capacity to donate electrons. Indeed, IE is linearly correlated with $-\Delta E_{BDE}$ with a relatively large correlation coefficient ($R^2 = 0.91$ for BF_3 and 0.84 for BMe_3). Ligands like $Be(NHMe_2)_3$, Bediene, and CAAC have resulted in lower IE values in comparison to ligands such H_2O, NH_3, and PMe_3 (see Table S9). As a result, beryllium and carbene containing ligands have a higher capacity to donate electron density to BX_3, in agreement with more stabilizing values of $-\Delta E_{BDE}$.

The second correlation (Figure 8b) shows that smaller $HOMO_{ligand}$-$LUMO_{BX3}$ gaps (GAP_{H-L}) are linearly correlated with larger $-\Delta E_{BDE}$ ($R^2 = 0.85$ for BF_3 and 0.81 for BMe_3), which is not unexpected considering that the interaction between the $HOMO_{ligand}$ and the $LUMO_{BX3}$ is the most important in soft acid-base interactions. We calculated the hardness for the ligands and boranes to corroborate the validity of the hard and soft acids and bases (HSAB) principle by Pearson.[85–87] We found the following trend: Bpyr (1.5 eV) < $Be(NHMe_2)_3$ (1.9 eV) < Bediene (1.9 eV) < BMes (3.4 eV) < CAAC (4.0 eV) < PSC (4.0 eV) < NHC (4.1 eV) < PMe_3 (5.0 eV) < pyr (5.2 eV) < NH_3 (6.2 eV) < HNC (6.8 eV) < H_2O (7.0 eV) < HCN (8.2 eV) and BMe_3 (6.0 eV) < BF_3 (8.3 eV). Our results show that Lewis bases with hardnesses similar to those of Lewis acids are not the ones having larger bond dissociation energies. For example, HCN, H_2O, HNC, and NH_3 have hardness values similar to BX_3. However, the bond dissociation energies for these systems are the lowest among the series. Moreover, beryllium compounds,

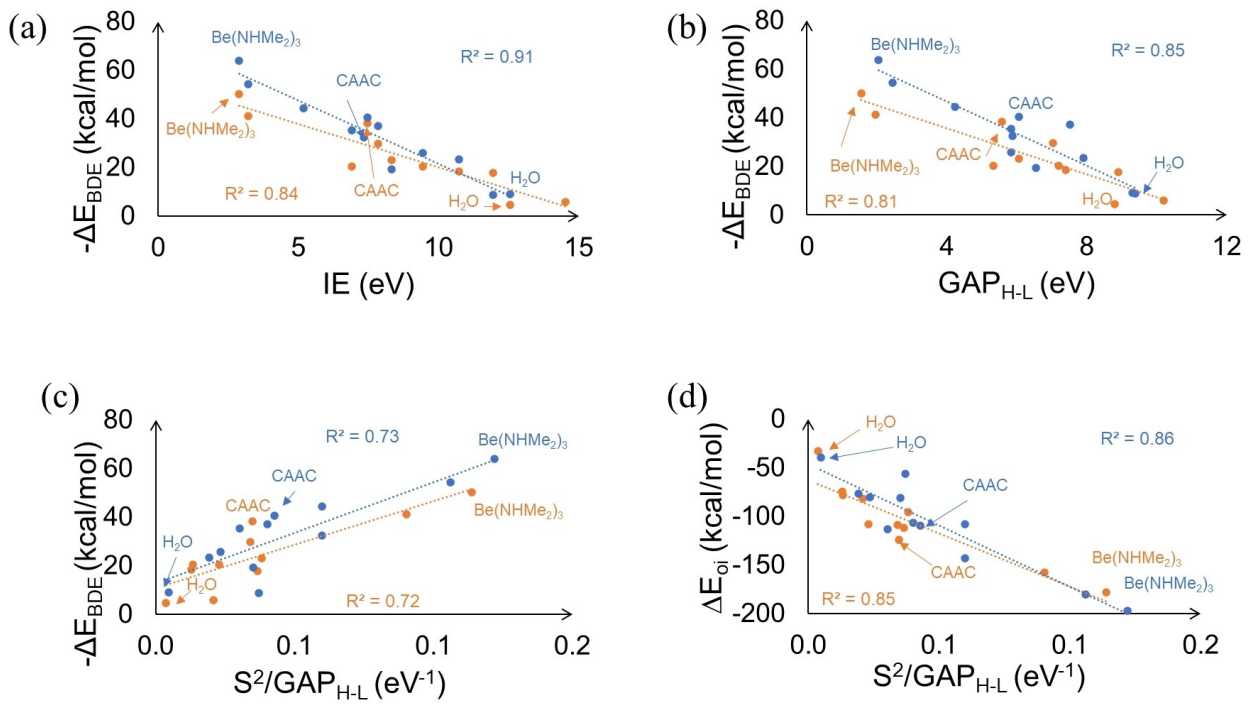

Figure 8. Correlations between (a) $-\Delta E_{BDE}$ and IE, (b) $-\Delta E_{BDE}$ and GAP_{H-L}, (c) $-\Delta E_{BDE}$ and S^2/GAP_{H-L} factor, and (d) ΔE_{oi} and S^2/GAP_{H-L} factor. Orange dots represent BMe_3 and blue dots represent BF_3 adducts.

Research Article
doi.org/10.1002/ejic.202200767

CAAC, and NHC despite their relatively low hardnesses resulted in an increased orbital interaction with the BX_3 moiety due to the decreased GAP_{H-L}. Several previous studies have also found failures of the HSAB principle.[88–90]

The perturbation molecular orbital theory suggests a possible correlation between the $-\Delta E_{BDE}$ and the S^2/GAP_{H-L}.[91] We checked this third correlation and we found that $-\Delta E_{BDE}$ has a lower correlation with S^2/GAP_{H-L} than with IE or GAP_{H-L}, but still a significant correlation exists ($R^2 = 0.72$, see Figure 8c). Not unexpectedly, correlation of S^2/GAP_{H-L} with ΔE_{oi} term ($R^2 = 0.85$, Figure 8d) is much better than with $-\Delta E_{BDE}$.

Finally, we analyzed a series of diborynes with a triple B≡B bond stabilized by some of the ligands studied. We selected four ligands of high, intermediate, and low $-\Delta E_{BDE}$ values, such as $Be(NHMe_2)_3$, CAAC, NH_3, and H_2O (see Figure 9 and Table S10). As compared to experimental values, the calculated B–B bond length in $(CAACB)_2$ differs by 0.027 Å and the L–B by 0.018 Å (*expt.* B–B 1.489 Å and L–B 1.458 Å[92]). For $(NH_3B)_2$, the B–B bond length is 1.424 Å only 0.002 Å shorter than a previous reported value (*theor.* 1.426 Å[93]). The $(NH_3B)_2$ MBO_{B-B} index is high (2.9), whereas the MBO_{L-B} (0.7) is low and suggests the possibility of NH_3 dissociation. Similarly, the MBO_{B-B} index for $(H_2OB)_2$ is high, but the MBO_{L-B} is low. On the other hand, the $(Be(NHMe_2)_3B)_2$ MBO_{L-B} (1.3) and $(CAACB)_2$ MBO_{L-B} (1.6) are above 1. We attribute this value higher than 1 to the important back-donation from the B to the $Be(NHMe_2)_3$ and CAAC ligands. Figure 9 shows the $\Delta G_{BDE:L-B}$ calculated using the Gibbs energies in DCM solvent as $-\Delta G_{BDE} = \Delta G_{BBtriplet}$[94] $+ 2\Delta G_L - \Delta G_{(LB)2}$ for each diboryne. As expected, NH_3 and H_2O ligands have the smallest values (46.4 kcal/mol for $(NH_3B)_2$ and 17.0 kcal/mol for $(H_2OB)_2$), whereas for $(Be(NHMe_2)_3B)_2$ and $(CAACB)_2$ the B–L dissociation energies are larger than 90.0 kcal/mol. These results suggest that weak σ-donor ligands result in L→B≡B←L diborynes that can decompose by losing the ligands at relatively low temperature. On the other hand, L→B≡B←L diborynes are particularly stabilized by medium and strong σ-donor ligands such $Be(NHMe_2)_3$, Bediene, BMpyr, CAAC, NHC or PSC ligands. It is worth noting that, as compared to CAAC, beryllium-based ligands lead to BB bonds with more triple bond character (MBO_{B-B} indices are 1.5 for CAAC and 2.2 for $Be(NHMe_2)_3$). Because of this particular behaviour, it is likely that beryllium-based ligands may stabilize triple B≡B bonds without reducing the efficiency of these species as metallomimetic catalysts for the activation of chemical bonds. For this reason, these ligands look very promising.

Conclusions

Diborenes and diborynes, which contain boron-boron multiple bonds, are stabilized by σ-donor ligands that provide electron density to these electron-deficient species. In this work, we used density functional calculations to determine the basicity of a series of σ-donor ligands. Our aim was to identify optimal σ-donor ligands to stabilize boron-boron multiple bonds. To this end, we have performed an energy decomposition analysis of the bond dissociation energies ($-\Delta E_{BDE}$) of the L–B bond in model systems L→BX_3 (X=F and Me). The results of the dissociation energies allow us to classify the ligands in strong, medium, and weak Lewis bases. Larger bond dissociation energies of L→BF_3 as compared to L→BMe_3 are found despite the longer L–B bond length in L→BF_3. The larger bond dissociation energies of L→BF_3 can be explained by the more stabilizing interaction energy in these adducts. The longer L–B bond lengths in L→BF_3 species is due to the strain energy that is particularly larger for L→BF_3 at short L–B distances. For all the ligands studied, the energy decomposition analysis of the interaction energy indicates similar contributions of the orbital interaction and electrostatic terms stabilizing components of the interaction energy. The orbital interaction term comes mainly from the interaction between the HOMO of the ligand and the LUMO of the BX_3 compound. The ionization energy of the ligands shows a good correlation with the bond dissociation energy. Indeed, one of the main factors that determine the bond strength is the HOMO energy, which is naturally

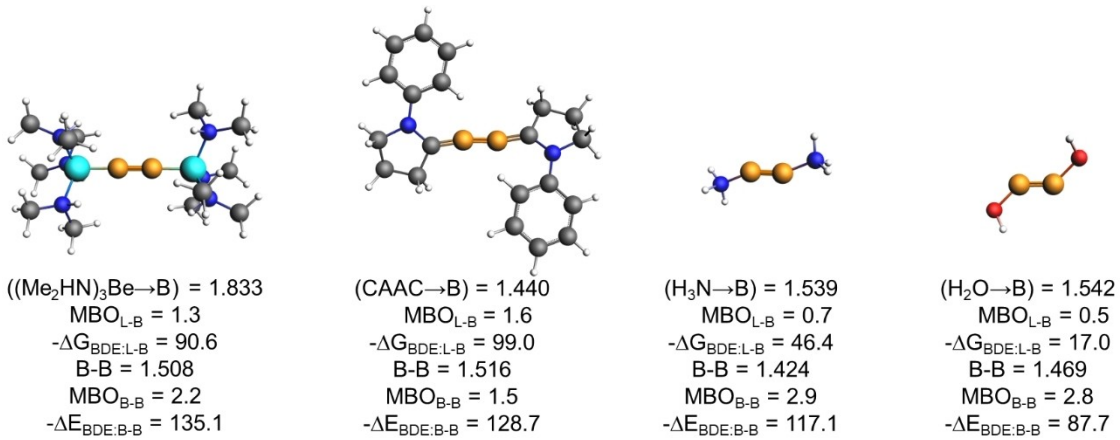

Figure 9. Diboryne compounds studied. L–B bond lengths in Å, Mayer bond orders (electrons), and bond dissociation energies $-\Delta E_{BDE}$ and $-\Delta G_{BDE}$ (in DCM) in kcal/mol. Grey: C, aqua: Be, white: H, blue: N, red: O, orange: B.

reflected by the ionization energy. Finally, we analysed the stability of some L→B≡B←L diborynes. Interestingly, we found that beryllium-based ligands stabilize the triple B≡B bonds of diborynes without reducing to a great extent the triple bond character of the B≡B bonds. We anticipate that this property could make L→B≡B←L diborynes more effective as metal-free catalysts for the activation of chemical bonds. Further research should be carried out to confirm our computationally guided insights concerning the properties of beryllium-based ligands.

Acknowledgements

D.E.T.G. would like to thank the DAIP and CONACYT for the fellowship (822937) and IQCC for the computational time in Beta Cluster and the fellowship provided by the GRCT090 group. M.S. thanks the Spanish Ministerio de Ciencia e Innovación for project PID2020-113711GB-I00 and the Generalitat de Catalunya for project 2021SGR623. T.A.H. and F.M.B. thank The Netherlands Organization for Scientific research (NWO) for financial support. J.O.C.J.-H. and M.S. acknowledge the Holland Research School of Molecular Chemistry (HRSMC) for a fellowship when visiting the TheoCheM group at Vrije Universiteit Amsterdam.

Conflict of Interest

The authors declare no conflict of interest.

Data Availability Statement

The data that support the findings of this study are available in the supplementary material of this article.

Keywords: boron · density functional theory · Lewis acids · Lewis bases · metallomimetic compounds · multiple bonds

[1] P. P. Power, *Nature* **2010**, *463*, 171–177.
[2] M. A. Légaré, C. Pranckevicius, H. Braunschweig, *Chem. Rev.* **2019**, *119*, 8231–8261.
[3] C. Weetman, *Chem. Eur. J.* **2021**, *27*, 1941–1954.
[4] A. Hofmann, M. A. Légaré, L. Wüst, H. Braunschweig, *Angew. Chem. Int. Ed.* **2019**, *58*, 9776–9781; *Angew. Chem.* **2019**, *131*, 9878–9883.
[5] D. Franz, T. Szilvási, A. Pöthig, S. Inoue, *Chem. Eur. J.* **2019**, *25*, 11036–11041.
[6] P. Vermeeren, M. T. Doppert, F. M. Bickelhaupt, T. A. Hamlin, *Chem. Sci.* **2021**, *12*, 4526–4535.
[7] K. D. Vogiatzis, M. V. Polynski, J. K. Kirkland, J. Townsend, A. Hashemi, C. Liu, E. A. Pidko, *Chem. Rev.* **2019**, *119*, 2453–2523.
[8] L. Grandell, A. Lehtilä, M. Kivinen, T. Koljonen, S. Kihlman, L. S. Lauri, *Renew. Energy* **2016**, *95*, 53–62.
[9] G. D. Frey, V. Lavallo, B. Donnadieu, W. W. Schoeller, G. Bertrand, *Science* **2007**, *316*, 439–441.
[10] Z. Zhu, X. Wang, Y. Peng, H. Lei, J. C. Fettinger, E. Rivard, P. P. Power, *Angew. Chem. Int. Ed.* **2009**, *48*, 2031–2034; *Angew. Chem.* **2009**, *121*, 2065–2068.
[11] D. E. Bergbreiter, J. M. Killough, *J. Am. Chem. Soc.* **1978**, *100*, 2126–2134.
[12] P. Bag, A. Porzelt, P. J. Altmann, S. Inoue, *J. Am. Chem. Soc.* **2017**, *139*, 14384–14387.
[13] A. N. Price, G. S. Nichol, M. J. Cowley, *Angew. Chem. Int. Ed.* **2017**, *56*, 9953–9957; *Angew. Chem.* **2017**, *129*, 10085–10089.
[14] J. Li, Z. Lu, L. L. Liu, *J. Am. Chem. Soc.* **2022**, *144*, 23691–23697.
[15] G. C. Welch, R. R. San Juan, J. D. Masuda, D. W. Stephan, *Science* **2006**, *314*, 1124–1126.
[16] D. W. Stephan, *Acc. Chem. Res.* **2015**, *48*, 306–316.
[17] D. W. Stephan, *Science* **2016**, *354*, aaf7229.
[18] J. J. Cabrera-Trujillo, I. Fernández, *Chem. Commun.* **2019**, *55*, 675–678.
[19] M. Ferrer, I. Alkorta, J. Elguero, J. M. Oliva-Enrich, *ChemPhysChem* **2022**, *23*, e202200204.
[20] B. Pachaly, R. West, *Angew. Chem. Int. Ed.* **1984**, *23*, 454–455; *Angew. Chem.* **1984**, *96*, 444–445.
[21] F. Fantuzzi, R. Moral, R. D. Dewhurst, H. Braunschweig, A. K. Phukan, *Chem. Eur. J.* **2022**, *28*, e202104123.
[22] H. Braunschweig, R. D. Dewhurst, *Organometallics* **2014**, *33*, 6271–6277.
[23] H. Braunschweig, I. Krummenacher, M. A. Legare, A. Matler, K. Radacki, Q. Ye, *J. Am. Chem. Soc.* **2017**, *139*, 1802–1805.
[24] Y. Ma, B. Wang, L. Zhang, Z. Hou, *J. Am. Chem. Soc.* **2016**, *138*, 3663–3666.
[25] Y. Wang, B. Quillian, P. Wei, C. S. Wannere, Y. Xie, R. B. King, H. F. Schaefer, P. v. R. Schleyer, G. H. Robinson, *J. Am. Chem. Soc.* **2007**, *129*, 12412–12413.
[26] Y. Wang, B. Quillian, P. Wei, Y. Xie, C. S. Wannere, R. B. King, H. F. Schaefer, P. v. R. Schleyer, G. H. Robinson, *J. Am. Chem. Soc.* **2008**, *130*, 3298–3299.
[27] M. Zhou, N. Tsumori, Z. Li, K. Fan, L. Andrews, Q. Xu, *J. Am. Chem. Soc.* **2002**, *124*, 12936–12937.
[28] M. Zhou, N. Tsumori, L. Andrews, Q. Xu, *J. Phys. Chem. A* **2003**, *107*, 2458–2463.
[29] A. Hermann, M. Arrowsmith, D. E. Trujillo-Gonzalez, J. O. C. Jiménez-Halla, A. Vargas, H. Braunschweig, *J. Am. Chem. Soc.* **2020**, *142*, 5562–5567.
[30] H. Braunschweig, R. D. Dewhurst, K. Hammond, J. Mies, K. Radacki, A. Vargas, *Science* **2012**, *336*, 1420–1422.
[31] R. Borthakur, K. Saha, S. Kar, S. Ghosh, *Coord. Chem. Rev.* **2019**, *399*, 213021.
[32] D. Auerhammer, M. Arrowsmith, P. Bissinger, H. Braunschweig, T. Dellermann, T. Kupfer, C. Lenczyk, D. K. Roy, M. Schäfer, C. Schneider, *Chem. Eur. J.* **2018**, *24*, 266–273.
[33] J. Böhnke, H. Braunschweig, T. Dellermann, W. C. Ewing, T. Kramer, I. Krummenacher, A. Vargas, *Angew. Chem. Int. Ed.* **2015**, *54*, 4469–4473; *Angew. Chem.* **2015**, *127*, 4551–4555.
[34] M. Arrowsmith, J. Böhnke, H. Braunschweig, M. A. Celik, T. Dellermann, K. Hammond, *Chem. Eur. J.* **2016**, *22*, 17169–17172.
[35] J. Böhnke, H. Braunschweig, T. Dellermann, W. C. Ewing, K. Hammond, J. O. C. Jimenez-Halla, T. Kramer, J. Mies, *Angew. Chem. Int. Ed.* **2015**, *54*, 13801–13805; *Angew. Chem.* **2015**, *127*, 14006–14010.
[36] M. Arrowsmith, J. Böhnke, H. Braunschweig, M. A. Celik, C. Claes, W. C. Ewing, I. Krummenacher, K. Lubitz, C. Schneider, *Angew. Chem. Int. Ed.* **2016**, *55*, 11271–11275; *Angew. Chem.* **2016**, *128*, 11441–11445.
[37] P. Bissinger, H. Braunschweig, K. Kraft, T. Kupfer, *Angew. Chem. Int. Ed.* **2011**, *50*, 4704–4707; *Angew. Chem.* **2011**, *123*, 4801–4804.
[38] P. Bissinger, H. Braunschweig, A. Damme, T. Kupfer, I. Krummenacher, A. Vargas, *Angew. Chem. Int. Ed.* **2014**, *53*, 5689–5693; *Angew. Chem.* **2014**, *126*, 5797–5801.
[39] X. Zhang, I. A. Popov, K. A. Lundell, H. Wang, C. Mu, W. Wang, H. Schnöckel, A. I. Boldyrev, K. H. Bowen, *Angew. Chem. Int. Ed.* **2018**, *57*, 14060–14064; *Angew. Chem.* **2018**, *130*, 14256–14260.
[40] N. Fedik, C. Mu, I. A. Popov, W. Wang, J. Wang, H. Wang, K. H. Bowen, A. I. Boldyrev, X. Zhang, *Chem. Eur. J.* **2020**, *26*, 8017–8021.
[41] C. Foroutan-Nejad, *J. Phys. Chem. A* **2021**, *125*, 1367–1373.
[42] L. Zhu, R. Kinjo, *Angew. Chem. Int. Ed.* **2022**, *61*, e202207631.
[43] A. Beste, O. Krämer, A. Gerhard, G. Frenking, *Eur. J. Inorg. Chem.* **1999**, *1999*, 2037–2045.
[44] D. Rodrigues Silva, L. Azevedo Santos, M. P. Freitas, C. Fonseca Guerra, T. A. Hamlin, *Chem. Asian J.* **2020**, *15*, 4043–4054.
[45] M. Lein, G. Frenking, *Theory and Applications of Compututational Chemistry. The first forty years* (Eds.: C. E. Dykstra, G. Frenking, K. S. Kim, G. E. Scuseria), Elsevier, Dordrecth **2005**, pp. 291–372.
[46] J. Vignolle, X. Cattoën, D. Bourissou, *Chem. Rev.* **2009**, *109*, 3333–3384.
[47] S. De, P. Parameswaran, *Dalton Trans.* **2013**, *42*, 4650–4656.
[48] A. J. Kalita, S. S. Rohman, C. Kashyap, S. S. Ullah, L. J. Mazumder, A. K. Guha, *ChemistrySelect* **2020**, *5*, 8798–8805.
[49] M. Calligaris, *Coord. Chem. Rev.* **2004**, *248*, 351–375.
[50] M. Ernzerhof, G. E. Scuseria, *J. Chem. Phys.* **1999**, *110*, 5029–5036.

Research Article
doi.org/10.1002/ejic.202200767

[51] G. te Velde, F. M. Bickelhaupt, E. J. Baerends, C. Fonseca Guerra, S. J. A. A. van Gisbergen, J. G. Snijders, T. Ziegler, *J. Comput. Chem.* **2001**, *22*, 931–967.
[52] C. Fonseca Guerra, J. G. Snijders, G. te Velde, E. J. Baerends, *Theor. Chem. Acc.* **1998**, *99*, 391–403.
[53] S. Grimme, J. Antony, S. Ehrlich, H. Krieg, *J. Chem. Phys.* **2010**, *132*, 154104.
[54] E. R. Johnson, A. D. Becke, *J. Chem. Phys.* **2005**, *123*, 024101.
[55] P. Vermeeren, S. C. C. van der Lubbe, C. Fonseca Guerra, F. M. Bickelhaupt, T. A. Hamlin, *Nat. Protoc.* **2020**, *15*, 649–667.
[56] M. Bickelhaupt, *J. Comput. Chem.* **1999**, *20*, 114–128.
[57] W. J. Van Zeist, F. M. Bickelhaupt, *Org. Biomol. Chem.* **2010**, *8*, 3118–3127.
[58] F. M. Bickelhaupt, E. J. Baerends, *Reviews in Computational. Chemistry* (Eds.: K. B. Lipkowitz, D. B. Boyd), Wiley-VCH, New York **1999**, pp. 1–86.
[59] A. Klamt, *WIREs Comput. Mol. Sci.* **2011**, *1*, 699–709.
[60] T. A. Hamlin, P. Vermeeren, C. Fonseca Guerra, F. M. Bickelhaupt, *Complementary Bonding Analysis* (Ed.: S. Grabowsky), De Gruyter, Berlin **2021**, pp. 199–212.
[61] C. Riplinger, F. Neese, *J. Chem. Phys.* **2013**, *138*, 034106.
[62] M. Saitow, U. Becker, C. Riplinger, E. F. Valeev, F. Neese, *J. Chem. Phys.* **2017**, *146*, 164105.
[63] F. Neese, F. Wennmohs, U. Becker, C. Riplinger, *J. Chem. Phys.* **2020**, *152*, 224108.
[64] R. Shankar, K. Senthilkumar, P. Kolandaivel, *Int. J. Quantum Chem.* **2009**, *109*, 764–771.
[65] I. Mayer, *Chem. Phys. Lett.* **1983**, *97*, 270–274.
[66] J. Monot, L. Fensterbank, M. Malacria, E. Laco¸te, S. J. Geib, D. P. Curran, *Beilstein J. Org. Chem.* **2010**, *6*, 709–712.
[67] T. Böttcher, S. Steinhauer, L. C. Lewis-Alleyne, B. Neumann, H. G. Stammler, B. S. Bassil, G. V. Röschenthaler, B. Hoge, *Chem. Eur. J.* **2015**, *21*, 893–899.
[68] K. Iijima, T. Noda, M. Maki, T. Sasase, S. Shibata, *J. Mol. Struct.* **1986**, *144*, 169–179.
[69] K. Töpel, K. Hensen, J. W. Bats, *Acta Crystallogr. Sect. C* **1984**, *40*, 828–830.
[70] V. Jonas, G. Frenking, M. T. Reetz, *J. Am. Chem. Soc.* **1994**, *116*, 8741–8753.
[71] J. Burt, J. W. Emsley, W. Levason, G. Reid, I. S. Tinkler, *Inorg. Chem.* **2016**, *55*, 8852–8864.
[72] D. Mootz, M. Steffen, *ZAAC - J. Inorg. Gen. Chem.* **1981**, *483*, 171–180.
[73] I. Krossing, I. Raabe, *J. Am. Chem. Soc.* **2004**, *126*, 7571–7577.
[74] M. E. Jacox, K. K. Irikura, W. E. Thompson, *J. Chem. Phys.* **2000**, *113*, 5705–5715.
[75] R. C. Haddon, *J. Phys. Chem. A* **2001**, *105*, 4164–4165.
[76] C. Laurence, J. F. Gal, *Lewis Basicity and Affinity Scales: Data and Measurement*, John Wiley & Sons, Chichester **2009**.
[77] M. Sana, G. Leroy, C. Wilante, *Organometallics* **1992**, *11*, 781–787.
[78] S. Sarmah, A. K. Guha, A. K. Phukan, *Eur. J. Inorg. Chem.* **2013**, *13*, 3233–3239.
[79] P. Kaszynski, S. Pakhomov, M. E. Gurskii, S. Y. Erdyakov, Z. A. Starikova, K. A. Lyssenko, M. Y. Antipin, V. G. Young, Y. N. Bubnov, *J. Org. Chem.* **2009**, *74*, 1709–1720.
[80] S. Berski, Z. Latajka, A. J. Gordon, *New J. Chem.* **2011**, *35*, 89–96.
[81] F. Bessac, G. Frenking, *Inorg. Chem.* **2006**, *45*, 6956–6964.
[82] S. Mebs, J. Beckmann, *J. Phys. Chem. A* **2017**, *121*, 7717–7725.
[83] D. A. Spiegel, K. B. Wiberg, L. N. Schacherer, M. R. Medeiros, J. L. Wood, *J. Am. Chem. Soc.* **2005**, *127*, 12513–12515.
[84] G. Skara, B. Pinter, J. Top, P. Geerlings, F. De Proft, F. De Vleeschouwer, *Chem. Eur. J.* **2015**, *21*, 5510–5519.
[85] R. G. Pearson, *J. Am. Chem. Soc.* **1963**, *85*, 3533–3539.
[86] R. G. Pearson, *J. Chem. Educ.* **1968**, *45*, 581.
[87] R. G. Pearson, *Chemical Hardness: Applications from Molecules to Solids*, Wiley, Weinheim **2005**.
[88] M. Breugst, H. Zipse, J. P. Guthrie, H. Mayr, *Angew. Chem. Int. Ed.* **2010**, *49*, 5165–5169; *Angew. Chem.* **2010**, *122*, 5291–5295.
[89] H. Mayr, M. Breugst, A. R. Ofial, *Angew. Chem. Int. Ed.* **2011**, *50*, 6470–6505; *Angew. Chem.* **2011**, *123*, 6598–6634.
[90] T. Bettens, M. Alonso, F. De Proft, T. A. Hamlin, F. M. Bickelhaupt, *Chem. Eur. J.* **2020**, *26*, 3884–3893.
[91] T. A. Albright, J. K. Burdett, M.-H. Whangbo, *Orbital Interactions in Chemistry*, John Wiley & Sons, Inc., Hoboken, NJ, USA **2013**.
[92] J. Böhnke, H. Braunschweig, W. C. Ewing, C. Hörl, T. Kramer, I. Krummenacher, J. Mies, A. Vargas, *Angew. Chem. Int. Ed.* **2014**, *53*, 9082–9085; *Angew. Chem.* **2014**, *126*, 9228–9231.
[93] S. Zilberg, J. Sivan, *J. Coord. Chem.* **2018**, *71*, 2053–2064.
[94] The ground state for B_2 is a triplet state, the singlet state being 24.9 kcal/mol higher in energy, see: S. Zilberg, M. Zinigrad, *Molecules* **2021**, *26*, 6428.

Manuscript received: December 13, 2022
Revised manuscript received: December 30, 2022
Accepted manuscript online: January 5, 2023

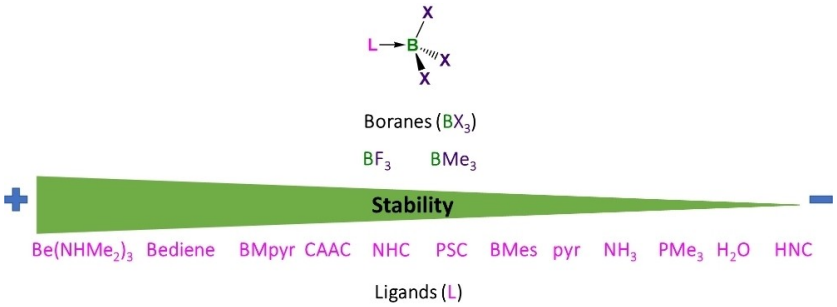

We use density functional calculations to determine the basicity of a series of σ-donor ligands with the aim to identify optimal σ-donor ligands to stabilize boron-boron multiple bonds. Beryllium-based ligands were found to stabilize the triple B≡B bonds of diborynes without reducing to a great extent their triple bond character.

D. E. Trujillo-González, Dr. G. González-García, Dr. T. A. Hamlin, Prof. Dr. F. M. Bickelhaupt, Prof. Dr. H. Braunschweig, Dr. J. O. C. Jiménez-Halla, Prof. Dr. M. Solà**

1 – 12

The Search for Enhanced σ-Donor Ligands to Stabilize Boron-Boron Multiple Bonds